Photon echoes and related four-wave-mixing spectroscopies using phase-locked pulses

Minhaeng Cho, Norbert F. Scherer, and Graham R. Fleming
Department of Chemistry and the James Frank Institute, The University of Chicago, Chicago, Illinois 60637

Shaul Mukamel
Department of Chemistry, University of Rochester, Rochester, New York 14627

(Received 3 December 1991; accepted 6 January 1992)

The use of phase-locked pulses in various spectroscopic techniques related to the third-order polarization $P^{(3)}$ is analyzed. Using correlation function expressions for the nonlinear response function, we clarify the interrelationship among several photon echo, pump–probe, and spontaneous light emission techniques, without alluding to any specific model for the material system. By combining phase-locked pulses and heterodyne detection it becomes possible to probe separately the real and imaginary parts of the nonlinear response function. Combining two phase-locked pulse excitation with time-resolved detection of the spontaneous light emission allows direct separation of the Raman and fluorescence contributions.

I. INTRODUCTION

The optical line shapes of molecular systems in condensed media are usually broadened by the large distribution of inhomogeneous environments representing the variation of the local solvent structure.[1-3] This dominant broadening mechanism often makes it impossible to probe molecular dynamics and optical dephasing processes using ordinary absorption spectroscopy and line shapes. Nonlinear optical spectroscopies such as photon echoes,[3-10] fluorescence line narrowing,[11] hole burning,[12] and pump–probe absorption[13-20] are commonly used to eliminate the inhomogeneous broadening effect, thereby allowing investigation of the electronic dephasing process in condensed media.

In hole burning and fluorescence line-narrowing experiments, the elimination of inhomogeneous broadening is achieved by a selective excitation of a subgroup of molecules using a narrow band excitation, and then following its subsequent dynamics. In contrast, the broadband pulsed excitation in photon echo spectroscopy is nonselective and usually the entire inhomogeneous distribution is excited. The ability of the echo technique to eliminate inhomogeneous contributions to the signal is the result of a combined effect of two carefully designed periods of evolution where the optical dephasing in the first period is followed by a rephasing process in the second period, resulting in the elimination of inhomogeneous broadening effect. Inhomogeneous broadening and dephasing are emsemble effects; the variation in the local environments of the chromophores alter the individual optical transition frequencies. Homogeneous line broadening and dephasing processes, by contrast, interrupt the individual chromophore phase evolution and result in irreversible loss of coherence in the emsemble.

A shortcoming of the conventional two-pulse and stimulated photon echo techniques resides in the detection of the intensity as opposed to the amplitude of the echo. Measurement of the echo amplitude would linearize the signal detection, as is the case for pump–probe spectroscopies that detect the pump–modified probe beam. This is especially of significance when examining the dynamics of dilute[14,15] and/or weakly absorbing chromophores.[18(a)] Such a linearized echo signal may be achieved by optical phase sensitive detection.[16(b),17] In principle, amplitude detection will allow measurement of the real and imaginary portions of echo field and the corresponding absorptive and dispersive portions of the optically induced material response. Two considerations are essential for phase-sensitive echo detection: (i) the echo signal is obtained following two periods of electronic phase evolution between time-separated optical pulses, and (ii) because of rapid phase modulation these periods are necessarily short for chromophores in liquid media. Therefore, an approach is required to maintain the relative phases between the short optical pulses used to create and detect the photon echo signal.

The ability to control the relative phases of pairs of femtosecond duration optical pulses[21] has created numerous new possibilities of novel nonlinear measurements. Recently Scherer *et al.*[22] studied the spontaneous light emission of Iodine in the gas phase, following an excitation by a phase-locked pulse pair. These two-pulse phase-locked interference measurements, performed on I_2 vapor, were shown to be very sensitive to the optical transition energies and the potential-energy surface of the excited state.[22,23] Conceptually, this approach is a time domain analog of a Young's two-slit interference experiment where only one interaction occurs with each of the two fields. The measured two-pulse interference contribution to the excited state populations at a given time delay reflects the phase and magnitude of the instantaneous transition dipole moment of the molecule.

Nonlinear spectroscopic techniques are most conveniently classified by expanding the optical polarization in powers of the applied field, $E(\mathbf{r},t)$,[24,25]

$$P(\mathbf{r},t) = P^{(1)}(\mathbf{r},t) + P^{(2)}(\mathbf{r},t) + P^{(3)}(\mathbf{r},t) + \cdots . \quad (1)$$

Spontaneous light emission (SLE) may also be described

 0021-9606/92/085618-12$06.00

using the third-order polarization $P^{(3)}$.[26(a)] The same nonlinear polarization is also responsible for numerous other four-wave mixing and related spectroscopies such as photon echo, pump probe, CARS, hole burning, etc.[26]

In this paper we explore the use of phase-locked pulses in several nonlinear optical measurements and analyze them from a unified theoretical viewpoint based on the nonlinear response function.[26,27] Generally, specific experiments will usually probe only parts of the total response function.[10] The calculation of a specific nonlinear measurement usually requires only a few of the individual Liouville space pathways (see below) which are complex (i.e., have real and imaginary parts) rather than the entire response function which is real. It is possible to calculate the complex nonlinear susceptibility of the system by Fourier transform of the time-dependent complex individual contributions to the complete nonlinear response functions.[27(a)]

The main goal of this paper is to show how the real and imaginary contributions to the response function can be measured separately using phase-locking techniques. We give a theoretical description of photon echo and pump–probe spectroscopy employing *phase-locked pulses*. We show that the phase-locking approach is particularly useful for measuring the complex nonlinear response functions associated with the photon echo and pump–probe absorption experiments. In general, by controlling the phase factor between the two pulses to be in-phase and in-quadrature, one obtains the imaginary and real parts of the nonlinear response functions. We present the direct relationships between the various photon echo and pump–probe experiments. We also discuss the utility of the phase-locked pump–probe absorption measurement for examining the optical dephasing processes. Finally, we show how the time-dependent detection of spontaneous light emission from a chromophore interacting with a phase-locked pulse pair allows us to obtain detailed information on the individual contributions to the nonlinear response function. Our results are summarized in Sec. VI.

II. NONLINEAR RESPONSE FUNCTION DESCRIPTION OF THE THIRD-ORDER POLARIZATION

In general, for systems consisting of a collection of dilute noninteracting chromophores, $P^{(3)}$ can be calculated using the nonlinear material response function $R(t_3,t_2,t_1)$,

$$P^{(3)}(\mathbf{r},t) = \int_0^\infty dt_1 \int_0^\infty dt_2 \int_0^\infty dt_3 R(t_3,t_2,t_1) \times E(\mathbf{r},t-t_3)E(\mathbf{r},t-t_3-t_2) \times E(\mathbf{r},t-t_3-t_2-t_1). \quad (2)$$

All the quantities appearing in this equation, $P^{(3)}$, E, and R are real.

For any combination of pulses, some of the terms in $P^{(3)}$ will contain differences of optical and electronic transition frequencies and others will contain sums of these frequencies. The later type of terms will be highly oscillatory and upon performing the time integrations will have a negligible contribution to the signal. Neglecting these terms is called the rotating wave approximation. When R is calculated by expanding the density matrix we find that it contains four basic terms corresponding to distinct Liouville space pathways,[26,27]

$$R(t_3,t_2,t_1) \equiv [R_1(t_3,t_2,t_1) + R_4(t_3,t_2,t_1)]\chi(t_1+t_3) + [R_2(t_3,t_2,t_1) + R_3(t_3,t_2,t_1)]\chi(t_1-t_3) + \text{c.c.} \quad (3)$$

Here the molecular response function is factorized into dynamic and static (i.e., inhomogeneous) contributions denoted by $R_\alpha(t_3,t_2,t_1)$ and $\chi(t)$, respectively.[10,27(b)] The individual contributions to the nonlinear response functions $R_\alpha(t_3,t_2,t_1)$ and $\chi(t)$ are complex, while the total response function R is real. $\chi(t)$ is given by the Fourier transform of the inhomogeneous distribution, $\hat{\chi}(\omega)$, of the optical transition frequencies of the chromophore

$$\chi(t) \equiv \int_{-\infty}^{\infty} d\omega \exp(-i\omega t)\hat{\chi}(\omega). \quad (4)$$

The other factors $R_\alpha(t_3,t_2,t_1)$ represent all other dynamical contributions to the response function. The four contributions to the molecular nonlinear response functions are given by[26(b)]

$$\begin{aligned} R_1(t_3,t_2,t_1) &= \mathrm{Tr}[G_{eg}(t_3)G_{ee}(t_2)G_{eg}(t_1)\rho_g], \\ R_2(t_3,t_2,t_1) &= \mathrm{Tr}[G_{eg}(t_3)G_{ee}(t_2)G_{ge}(t_1)\rho_g], \\ R_3(t_3,t_2,t_1) &= \mathrm{Tr}[G_{eg}(t_3)G_{gg}(t_2)G_{ge}(t_1)\rho_g], \\ R_4(t_3,t_2,t_1) &= \mathrm{Tr}[G_{eg}(t_3)G_{gg}(t_2)G_{eg}(t_1)\rho_g]. \end{aligned} \quad (5)$$

We assume that the system is initially in thermal equilibrium in the electronic ground state with density matrix ρ_g. Tr denotes a trace over the nuclear degrees of freedom including both the solvent and the chromophore. The Green's function, $G_{mn}(t)$, is defined by the action on an arbitrary operator A,

$$G_{mn}(t)A = \exp(-iH_m t)A\exp(iH_n t), \quad m,n = e,g, \quad (6)$$

where H_g and H_e are the adiabatic Hamiltonians characterizing the nuclear degrees of freedom of the entire molecular system (solute and solvent) in electronic states $|g\rangle$ and $|e\rangle$, respectively. Thus, both multilevel intramolecular processes and solvation dynamics are explicitly included. Each of the four contributions represents a different sequence of time evolutions of the density matrix, denoted "Liouville space pathways." We shall later explore the nature of these pathways in the context of specific nonlinear techniques.

In the most general four-wave-mixing measurement, the external field is given by

$$E(\mathbf{r},t) = E_1(t+\tau'+\tau)\exp(i\mathbf{k}_1\mathbf{r} - i\omega_1 t) + E_2(t+\tau)\exp(i\mathbf{k}_2\mathbf{r} - i\omega_2 t) + E_3(t)\exp(i\mathbf{k}_3\mathbf{r} - i\omega_3 t) + \text{c.c.}, \quad (7)$$

where $E_i(t)$ and ω_i denote the temporal amplitude and mean frequency of the ith incident pulse. The first, second, and third fields E_1, E_2, and E_3 peak at times $-(\tau+\tau')$, $-\tau$, and 0, respectively. τ and τ' are the relative delays of the pulses. The nonlinear polarization $P^{(3)}$ is similarly expanded,

$$P(\mathbf{r},t) = \sum_s P(\mathbf{k}_s,t)\exp(i\mathbf{k}_s\mathbf{r} - i\omega_s t) + \text{c.c.}, \quad (8)$$

where $\mathbf{k}_s$ can be any combination of the incoming wave vectors, $\mathbf{k}_s = \pm\mathbf{k}_1 \pm \mathbf{k}_2 \pm \mathbf{k}_3$ and $\omega_s = \pm\omega_1 \pm \omega_2 \pm \omega_3$. The various experimental techniques differ by the choice of $\mathbf{k}_s$ and the timing of the incoming pulses.

Assuming that the pulses are infinitely short, the triple integration in Eq. (2) can be trivially carried out. Equations (2) and (3) then result in $P^{(3)}(\mathbf{r},t) \sim R(t,\tau,\tau')$. In this case, therefore, $P^{(3)}$ is directly proportional to the total nonlinear response function $R(t_3,t_2,t_1)$. In practice, even for impulsive experiments involving femtosecond pulses, the pulses may be short compared to molecular relaxation and dynamic time scales but not compared with the optical frequency. In fact, in order to define a short light pulse, the pulses have always to be long compared with the optical frequency. The fact that the light pulses are not simply mathematical δ functions has some important consequences.

III. NONLINEAR RESPONSE FUNCTION REPRESENTATION OF PHOTON ECHO MEASUREMENTS

In this section we will survey the general features of photon echo generation for various pulse trains (see Fig. 1), following the Liouville space response function formulation of Yan and Mukamel.[10,27(a)] These descriptions of photon echo techniques that lack phase control will subsequently be compared with a theoretical formulation of the heterodyne-detected stimulated photon echo (HSPE) generated and measured by using *phase-controlled pulse pairs* (Sec. IV), with the phase-locked pump–probe (PL-PP) absorption using three pulses (Sec. V), and with the spontaneous light emission signal obtained using a phase-locked pulse pair (PL-SLE) (Sec. VI).

The most general configuration of the external fields in photon echo measurements involves three pulses having three different wave vectors and frequencies and separated by time delays τ' and τ [Eq. (7)]. This scheme results in a detected (fourth) field with wave vector $\mathbf{k}_s = \mathbf{k}_3 + \mathbf{k}_2 - \mathbf{k}_1$ that is usually termed a stimulated photon echo (SPE). The photon echo signal is produced at time $t \cong \tau'$ after the chromophore interacts with the third pulse, where τ' is identical to the delay time between the first and second pulses. The double-sided Feynman diagrams that contribute to the $\mathbf{k}_s$ polarization are shown in Fig. 2. Pathways R_1 and R_2 describe the population relaxation and the evolution of vibra-

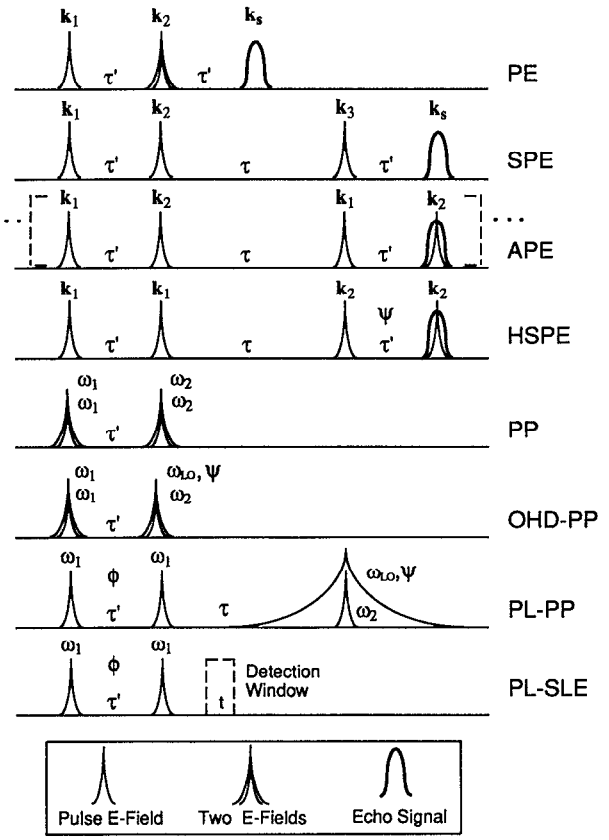

FIG. 1. Pulse sequences for the various $P^{(3)}$ techniques considered here. PE, photon echo; SPE, stimulated photon echo; APE, accumulated photon echo; HSPE, heterodyne-detected stimulated photon echo; PP, pump-probe; OHD-PP, optical heterodyne-detected pump–probe; PL-PP, phase-locked pump–probe; PL-SLE, phase-locked spontaneous light emission. In APE and HSPE, the fourth pulse coincides spatially and temporally with the echo signal. The phase relations between the two consecutive pulses are adjusted as ϕ or ψ in HSPE, PL-PP, and PL-SLE. On the other hand, the optical phase of the local oscillator (of frequency, ω_{LO}) is described as ψ in OHD-PP and PL-PP.

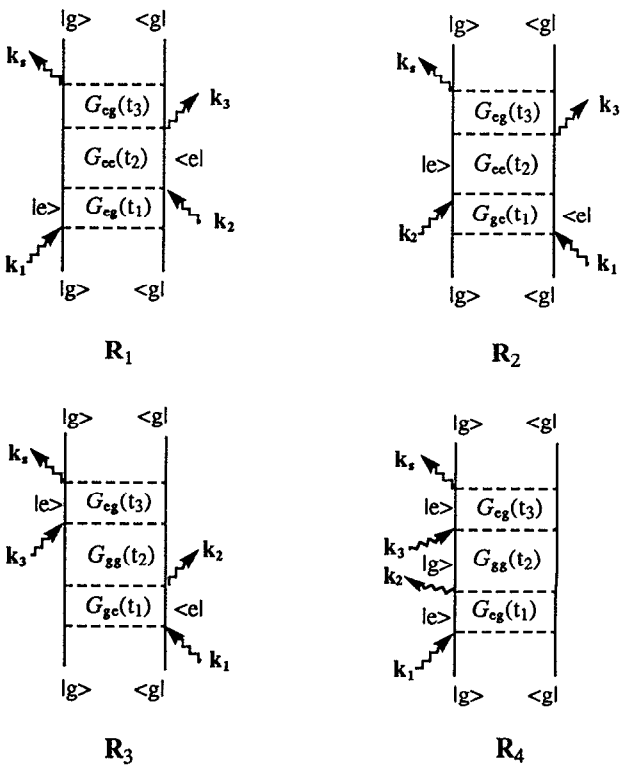

FIG. 2. Double-sided Feynman diagrams for the stimulated photon echo in the rotating wave approximation. The diagram denoted as R_α represents the molecular nonlinear response functions $R_\alpha(t_3,t_2,t_1)$ in Eqs. (3) and (5). In a Feynman diagram the left (right) vertical line represent the ket (bra) propagation of the density matrix. The wavy arrows denote interactions with the external fields. The time runs from bottom to top. The system is initially at thermal equilibrium in the electronic ground state, $|g\rangle\langle g|$. Between interactions, the system evolves according to the Green's functions defined in Eq. (6).

tional coherence in the electronically excited state, while R_3 and R_4 are associated with the ground state dynamics.

As discussed in Sec. II, $\chi(t)$ is given by the Fourier transform of the inhomogeneous distribution, $\hat{\chi}(\omega)$, of the optical transition frequencies of the chromophore. Thus, a broad distribution for $\hat{\chi}(\omega)$ results in only the pathways R_2 and R_3 contributing to the rephasing processes generating the echo signal; $\chi(t)$ is effectively a δ function. The time arguments appearing in the χ functions appropriate to R_1 and R_2, for example, differ in sign depending on whether the two interactions bracketing the t_2 period (i.e., excited state population in these cases) act consecutively on one or alternate sides of the diagram (see Fig. 2). The $\chi(t_3 - t_1)$ factor appearing in the R_2 and R_3 contributions will create a strong peak (echo) at $t_1 = t_3$. The $\chi(t_3 + t_1)$ factor in the R_1 and R_4 pathways could only peak at $t_1 = t_3 = 0$ (since t_1 and t_3 are positive) and will not contribute to the echo.

A. Stimulated photon echo

Invoking the rotating wave approximation and assuming that the excitation pulses are well separated, the stimulated photon echo signal is then given by[10]

$$S_{\mathrm{SPE}}(\tau',\tau) = \int_0^\infty dt\, |P^{(3)}_{\mathrm{SPE}}(\mathbf{k}_s,t)|^2, \tag{9}$$

where the macroscopic polarization, $P^{(3)}_{\mathrm{SPE}}(\mathbf{k}_s,t)$, is described by

$$\begin{aligned} P^{(3)}_{\mathrm{SPE}}(\mathbf{k}_s,t) = -i \int_0^\infty dt_3 \int_0^\infty dt_2 \int_0^\infty dt_1 \{ & [R_2(t_3,t_2,t_1) + R_3(t_3,t_2,t_1)] \\ & \times \chi(t_3 - t_1) E_3(t - t_3) E_2(t + \tau - t_3 - t_2) E_1^*(t + \tau + \tau' - t_3 - t_2 - t_1) \\ & \times \exp[i(\omega_3 + \omega_2 - \omega_1 - \omega_{eg})t_3 + i(\omega_2 - \omega_1)t_2 - i(\omega_1 - \omega_{eg})t_1] \}. \end{aligned} \tag{10}$$

The dynamical information contributing to the photon echo signal is fully contained in the molecular nonlinear response functions R_2 and R_3. We should note that these are the same nonlinear response functions used in describing the pump–probe absorption in the large inhomogeneous broadening limit[10] (see the following).

The physical process described by Eq. (10) and shown as SPE in Fig. 1 may be understood as the following. An optical coherence state is produced by the interaction of the chromophore with the first field at time $t \cong -(\tau' + \tau)$. The system then evolves according to the off-diagonal Green's functions (time-evolution operators) for approximately τ' (approximately because of finite pulse duration). The second interaction at $t \cong -\tau$ with the second field produces populations in either the ground or excited electronic states. The population developed by consecutive interactions with the two fields evolves on the potential surfaces of the electronic ground or excited states. During the time period τ, we may observe vibrational coherences (i.e., quantum beats) in the ground or the excited states and pure population relaxation in the excited state. The third field, acting at $t \cong 0$, induces optical coherence again. Finally, the (three-pulse) stimulated photon echo signal is produced at time $t \cong \tau'$ by the rephasing process in the case of an inhomogeneously broadened medium. The ordinary two-pulse photon echo signal is obtained by $S_{\mathrm{PE}}(\tau') = S_{\mathrm{SPE}}(\tau', \tau = 0)$.

B. Accumulated photon echo

We now turn to the accumulated photon echo (see APE of Fig. 1).[3,6] In general, the accumulated photon echo is performed using two trains with many pulse pairs. The echo signal, however, requires only two pulses in each train, hence, the four-pulse sequence shown in Fig. 1. The trains simply serve to increase the signal by accumulating the contributions of many four-pulse sequences.

In contrast to the two-pulse photon echo and the stimulated photon echo signals the accumulated photon echo signal is detected by the interference of the third-order polarization ($\mathbf{k}_s = \mathbf{k}_1 + \mathbf{k}_2 - \mathbf{k}_1$) with the fourth (probe) field. Thus, the signal is given by[10]

$$S_{\mathrm{APE}}(\omega_1,\omega_2;\tau',\tau) = -2\,\mathrm{Im} \int_{-\infty}^{\infty} dt E_2^*(t - \tau') P^{(3)}_{\mathrm{SPE}}(\mathbf{k}_2,t) \tag{11}$$

$$\begin{aligned} = 2\,\mathrm{Re} \int_{-\infty}^{\infty} dt \int_0^\infty dt_3 \int_0^\infty dt_2 \int_0^\infty dt_1 \{ & [R_2(t_3,t_2,t_1) + R_3(t_3,t_2,t_1)] \chi(t_3 - t_1) \\ & \times E_2^*(t - \tau') E_1(t - t_3) E_2(t + \tau - t_3 - t_2) E_1^*(t + \tau + \tau' - t_3 - t_2 - t_1) \\ & \times \exp[i(\omega_2 - \omega_{eg})t_3 + i(\omega_2 - \omega_1)t_2 - i(\omega_1 - \omega_{eg})t_1] \}, \end{aligned} \tag{12}$$

where the response functions R_2 and R_3 were defined in Eq. (5). Here a complete cycle of four consecutive pulses, i.e., two from the pump train and two from the probe train, is considered.

C. Impulsive and inhomogeneous limits

Two approximations can be made to simplify the expressions for the echo signals. First, the impulsive limit is

obtained when the pulse durations are shorter than both (i) the molecular vibrational periods and (ii) the time scales of homogeneous dephasing and solvent reorganization processes (but not short compared to the period of one optical frequency). Second, we invoke the large inhomogeneous broadening limit, whereby the inhomogeneous dephasing time is short compared to all the other dynamical time scales of the system. Assuming these limits, the echo signals can be simplified to[10]

$$S_{\mathrm{PE}}(\tau') = |R_2(\tau',0,\tau') + R_3(\tau',0,\tau')|^2,$$
$$S_{\mathrm{SPE}}(\tau',\tau) = |R_2(\tau',\tau,\tau') + R_3(\tau',\tau,\tau')|^2, \qquad (13)$$
$$S_{\mathrm{APE}}(\tau',\tau) = \mathrm{Re}[R_2(\tau',\tau,\tau') + R_3(\tau',\tau,\tau')].$$

Although the general response function associated with all photon echo signals are basically identical, namely R_2 and R_3, each experiment only measures part of the full nonlinear response function. This limitation will be overcome by using optical heterodyne detection of the stimulated photon echo experiment as shown later.

IV. HETERODYNE-DETECTED STIMULATED PHOTON ECHO USING PHASE-LOCKED PULSES

A. Relation of HSPE to the conventional photon echoes

In the case of the accumulated photon echo, the third-order polarization produced by the three interactions with the external fields interferes with the fourth field. The accumulated photon echo signal is, therefore, directly proportional to the third-order polarization, whereas the two-pulse and stimulated photon echoes are proportional to square of the third-order polarization [compare Eq. (9) with Eq. (11)]. This linearization of the detection is very similar to optical heterodyne detection (OHD) in pump–probe experiments, in contrast to homodyne detection,[28] where the local oscillator field has the same wave vector as the probe field. In general, the homodyne detected signal can be expressed by

$$S_{\mathrm{homodyne}} \propto |\mathbf{E}_s|^2, \qquad (14)$$

while the heterodyne signal is

$$S_{\mathrm{heterodyne}} \propto 2\,\mathrm{Re}(\mathbf{E}_s\mathbf{E}_{\mathrm{LO}}). \qquad (15)$$

In principle, the magnitude of the local oscillator (LO) field can be adjusted to make the OHD signal large compared to the homodyne detected signal. Furthermore, it is possible to *selectively* measure the real and imaginary parts of the nonlinear response function by controlling the phase shift of the fourth field with respect to the third.

Here we describe a new technique, heterodyne-detected stimulated photon echo (HSPE) spectroscopy, that embodies the aforementioned advantages of the accumulated photon echo measurement. The HSPE approach involves only a single four-pulse sequence in contrast to the repetitive train of four pulses which create and detect accumulated photon echoes (see Fig. 1). The heterodyne-detected stimulated photon echo (HSPE) signal using phase-locked pulses is

$$\begin{aligned} S_{\mathrm{HSPE}}(\tau',\tau,\psi) &= -2\,\mathrm{Im}\int_{-\infty}^{\infty} dt E^*_{\mathrm{LO}}(t-\tau')P^{(3)}_{\mathrm{SPE}}(\mathbf{k}_2,t) \\ &= 2\,\mathrm{Re}\int_{-\infty}^{\infty} dt \int_0^{\infty} dt_3 \int_0^{\infty} dt_2 \int_0^{\infty} dt_1 \{[R_2(t_3,t_2,t_1) + R_3(t_3,t_2,t_1)]\chi(t_3-t_1) \\ &\quad \times E^*_{\mathrm{LO}}(t-\tau')E_2(t-t_3)E_1(t+\tau-t_3-t_2)E^*_1(t+\tau+\tau'-t_3-t_2-t_1) \\ &\quad \times \exp[i\psi + i(\omega_{\mathrm{LO}}-\omega_2)t + i(\omega_2-\omega_{eg})t_3 + i(\omega_2-\omega_1)t_2 - i(\omega_1-\omega_{eg})t_1]\}, \end{aligned} \qquad (16)$$

where $E_{\mathrm{LO}}(t)$ denotes the envelope of the local oscillator pulse. This expression is analogous to Eq. (12). Here, however, the phase shift, ψ, between the third (probe) and the fourth (local oscillator) fields is manifest in the exponential term of Eq. (16). Control of the relative phase of the third and fourth fields is the crucial factor in measuring the heterodyne-detected stimulated photon echo.

In the impulsive and the large inhomogeneous broadening limits we obtain

$$S_{\mathrm{HSPE}}(\tau',\tau,\psi) = 2\mathrm{Re}\{[R_2(\tau',\tau,\tau') + R_3(\tau',\tau,\tau')]\exp(i\psi)\exp[i(\omega_{\mathrm{LO}}-\omega_1)\tau' + i(\omega_2-\omega_1)\tau]\}. \qquad (17)$$

If $\omega_1 = \omega_2 = \omega_{\mathrm{LO}}$, then

$$S_{\mathrm{HSPE}}(\tau',\tau,\psi) = 2\mathrm{Re}\{[R_2(\tau',\tau,\tau') + R_3(\tau',\tau,\tau')]\exp(i\psi)\} = \begin{cases} 2Re[R_2(\tau',\tau,\tau') + R_3(\tau',\tau,\tau')] & \text{for } \psi = 0 \\ -2\mathrm{Im}[R_2(\tau',\tau,\tau') + R_3(\tau',\tau,\tau')] & \text{for } \psi = \pi/2 \end{cases}. \qquad (18)$$

Thus a complete record of the complex nonlinear response functions that describe echo generation can be obtained with a phase-controlled pulse pairs in the heterodyne-detected stimulated photon echo experiment. The real (imaginary) part of the nonlinear response functions is obtained from the in-phase (in-quadrature) HSPE. Using the full nonlinear response functions, we can similarly express all the other photon echoes in terms of the HSPE,

$$\begin{aligned} S_{\mathrm{PE}}(\tau') &= [S_{\mathrm{HSPE}}(\tau',\tau=0,\psi=0)]^2 \\ &\quad + [S_{\mathrm{HSPE}}(\tau',\tau=0,\psi=\pi/2)]^2, \\ S_{\mathrm{SPE}}(\tau',\tau) &= [S_{\mathrm{HSPE}}(\tau',\tau,\psi=0)]^2 \\ &\quad + [S_{\mathrm{HSPE}}(\tau',\tau,\psi=\pi/2)]^2, \\ S_{\mathrm{APE}}(\tau',\tau) &= S_{\mathrm{HSPE}}(\tau',\tau,\psi=0). \end{aligned} \qquad (19)$$

B. Relation of heterodyne-detected stimulated photon echo to pump–probe absorption

The pump–probe absorption signal is related to the photon echo as the frequency domain analog under some limiting conditions.[10] In this technique we need to consider $\mathbf{k}_s = \mathbf{k}_2 + \mathbf{k}_1 - \mathbf{k}_1$. Assuming both the large inhomogeneous broadening limit and the condition that the pump and probe pulses are short compared to the molecular nuclear dynamics and long compared to the electronic dephasing time, the pump–probe signal is given by [Eq. (13) in Ref. 10]

$$S_{PP}(\tau;\omega_2-\omega_1) = \mathrm{Re}\int_0^\infty dt \exp[i(\omega_2-\omega_1)t] \times [R_2(t,\tau,t) + R_3(t,\tau,t)]. \quad (20)$$

Thus, this pump–probe signal is directly related to the in-phase and in-quadrature HSPE signals by

$$\begin{aligned} S_{PP}(\tau;\omega_2-\omega_1) &\propto \mathrm{Re}\int_0^\infty dt \exp[i(\omega_2-\omega_1)t] \\ &\quad \times [S_{\mathrm{HSPE}}(t,\tau,\psi=0) \\ &\quad - iS_{\mathrm{HSPE}}(t,\tau,\psi=\pi/2)] \\ &= \int_0^\infty dt \cos[(\omega_2-\omega_1)t] \\ &\quad \times S_{\mathrm{HSPE}}(t,\tau,\psi=0) \\ &\quad + \int_0^\infty dt \sin[(\omega_2-\omega_1)t] \\ &\quad \times S_{\mathrm{HSPE}}(t,\tau,\psi=\pi/2). \end{aligned} \quad (21)$$

The two-pulse pump–probe signal is related to the HSPE as the Fourier–Laplace transform of the HSPE signals over the periods, τ', of the optical coherence states. Therefore, the two-pulse pump–probe signal (without frequency resolving the probe beam) cannot be used to investigate (fast) optical dephasing processes in condensed media.

V. THREE-PULSE PHASE-LOCKED PUMP–PROBE ABSORPTION

In this section we consider three-pulse pump–probe absorption with a pair of phase-locked pump pulses and optical heterodyne detection. The pulse train is shown in Fig. 1. The second pump pulse is delayed by τ' from the first and its phase factor, ϕ, is controlled relative to that of the first pump pulse. The probe pulse (and local oscillator pulse with phase factor ψ relative to the probe pulse) follows the second pump with time delay τ.

A. Nonlinear response function representation of phase-locked pump–probe absorption

The probe differential absorption measured by optical heterodyne detection is described by

$$S^{\mathrm{PL\text{-}PP}} = -2\,\mathrm{Im}\int_{-\infty}^{\infty} dt\, \mathbf{E}^*_{\mathrm{LO}}(t)\mathbf{P}^{(3)}_{\mathrm{PL\text{-}PP}}(\mathbf{k}_s,t), \quad (22)$$

where $\mathbf{P}^{(3)}_{\mathrm{PL\text{-}PP}}(\mathbf{k}_s = \mathbf{k}_2 + \mathbf{k}_1 - \mathbf{k}_1, t)$ represents the polarization induced in the optical medium through the third-order interaction with the phase-locked external fields.

Since we are using two pump pulses and a probe pulse to generate the nonlinear polarization, we may measure three contributions to the total integrated signal.

1. Contribution I, S_I

The chromophore interacts twice with the first pump pulse to create vibrational coherence and population in either the electronically ground or excited states. Then the third-order polarization produced by the interaction with the probe pulse at time $t \cong 0$ is detected by the fourth interaction with the local oscillator field. In this case the delay time between the pump and the probe pulses is given by $\tau + \tau'$.

2. Contribution II, S_{II}

The chromophore interacts twice with the second pump pulse and once with the probe pulse. The delay time between the two pulses (pump and probe) is given by τ. The nonlinear polarization is detected as in S_I.

3. Contribution III, S_{III}

In contrast to contributions S_I and S_{II}, which are independent of the phase factor ϕ, the third contribution is explicitly sensitive to it. In this contribution the chromophore interacts once with the first pump pulse to create an optical coherence state that evolves during the first time delay τ'. The optical coherence state is changed to either a population or a vibrational coherence in the electronically ground or excited state by a single interaction with the second pump pulse. The relative optical phase of the second pulse is controlled with respect to the first pump pulse. This phase-dependent features of these coherences and populations represents quantum-mechanical interference effects which have been studied experimentally and theoretically.[22,23] As before, the third-order polarization produced by the interaction with the probe pulse at time $t \cong 0$ is detected by the fourth interaction with the local oscillator field.

Hereafter, we only consider the signal generated by the third contribution, $S^{\mathrm{PL\text{-}PP}}_{\mathrm{III}}$, since it is the only phase-dependent contribution. That contribution can be measured by subtracting the signal obtained with each pump pulse individually from the total signal obtained with both phase-locked pump pulses. The first two contributions can be obtained by simply changing the phase factor and integrating $S^{\mathrm{PL\text{-}PP}}_{\mathrm{III}}$ over the first delay time, τ'.

The external fields that generate the third contribution are given by

$$\begin{aligned} E(\mathbf{r},t) &= E_1(t+\tau+\tau')\exp[i\mathbf{k}_1\mathbf{r} - i\omega_1 t] \\ &\quad + E_1(t+\tau)\exp[i\mathbf{k}_1\mathbf{r} - i\omega_1 t - i\phi] \\ &\quad + E_2(t)\exp[i\mathbf{k}_2\mathbf{r} - i\omega_2 t] + \mathrm{c.c.}, \end{aligned} \quad (23a)$$

$$E_{\mathrm{LO}}(\mathbf{r},t) = E_{\mathrm{LO}}(t)\exp[i\mathbf{k}_2\mathbf{r} - i\omega_{\mathrm{LO}}t - i\psi] + \mathrm{c.c.}, \quad (23b)$$

where $E_1(t+\tau+\tau')$, $E_1(t+\tau)$, $E_2(t)$, and $E_{LO}(t)$ are the temporal envelopes of the first pump, second pump, probe, and local oscillator fields, respectively. For simplicity we assume that the envelopes and frequencies of the two pump pulses are identical except for the phase-locking angle ϕ. The phase shift ψ of the local oscillator with respect to the third field (probe) is adjusted to fixed values of 0 or $\pi/2$ in Eq. (23b).

Invoking the rotating wave approximation and assuming the excitation pulses to be well separated, we obtain

$$\begin{aligned} S_{III}^{PL\text{-}PP}(\omega_1,\omega_2,\tau',\tau,\phi;\omega_{LO},\psi) = 2\,\mathrm{Re}\int_{-\infty}^{\infty} dt \int_0^{\infty} dt_3 \int_0^{\infty} dt_2 \int_0^{\infty} dt_1 \{ & [R_2(t_3,t_2,t_1) \\ & + R_3(t_3,t_2,t_1)]\chi(t_3-t_1)E_{LO}^{*}(t)E_2(t-t_3)E_1(t+\tau-t_3-t_2) \\ & \times E_1^{*}(t+\tau+\tau'-t_3-t_2-t_1) \\ & \times \exp[i(\omega_{LO}-\omega_2)t+i\psi+i(\omega_2-\omega_{eg})t_3-i(\omega_1-\omega_{eg})t_1-i\phi] \\ & + [R_1(t_3,t_2,t_1)+R_4(t_3,t_2,t_1)\chi(t_3+t_1) \\ & \times E_{LO}^{*}(t)E_2(t-t_3)E_1^{*}(t+\tau-t_3-t_2)E_1(t+\tau+\tau'-t_3-t_2-t_1) \\ & \times \exp[i(\omega_{LO}-\omega_2)t+i\psi+i(\omega_2-\omega_{eg})t_3+i(\omega_1-\omega_{eg})t_1+i\phi]\}. \end{aligned} \tag{24}$$

The pathways corresponding to the four response functions that contribute to the phase-locked pump–probe absorption signal are diagrammatically shown in Fig. 3.

The physical interpretation of Eq. (24) is the following. The system is prepared in a state of electronic coherence following the interaction with the first pulse at time $t \cong -(\tau+\tau')$. The system is then transferred to either the electronic ground-state population ρ_g or the excited state population ρ_e by the second interaction at $t \cong -\tau$. If two vibronic states in the ground (excited) state are coupled to the same vibronic state in the excited (ground) state via the radiation field, a vibrational coherence is created in the ground (excited) state. This may give rise to quantum beats in the signal. These vibrational nonstationary states evolve as described by the Green functions $G_{gg}(t)$ and $G_{ee}(t)$, respectively, until the system interacts with the third pulse (probe field). The third-order polarization produced by the consecutive interactions with the external fields, twice with the successive pump pulses and once with the probe pulse, is detected by the interference of the induced polarization with the fourth pulse (local oscillator). In particular, if we use a local oscillator field passing through the sample with the same wave vector as the polarization, whereby the frequency, phase factor, and amplitude of the local field can be arbitrarily controlled, we obtain the optical heterodyne-detected signal.

From Eq. (24) the conventional two-pulse pump–probe absorption can be obtained by integrating the signal from the third contribution,

$$S_{PP}(\omega_1,\omega_2;\tau) = \int_0^{\infty} d\tau' S_{III}^{PL\text{-}PP}(\omega_1,\omega_2,\tau',\tau,\phi=0;\omega_{LO}=\omega_2,\psi=0). \tag{25}$$

In the two-pulse pump–probe absorption, the optical coherence of the chromophore is produced by the first interaction with the pump field. The second interaction with the external field also occurs within the duration of the first pulse. Therefore, the population or the vibrational coherences in either the ground or excited states are produced by two interactions with the first pulse. However, the three-pulse phase-locked pump–probe absorption discussed earlier includes an additional time delay τ' between the first two interactions. A measurable PL-PP signal implies that the optical coherence state persists for a period of τ'. This is a distinctive feature of the PL-PP measurement.

B. Relation of phase-locked pump–probe absorption and heterodyne-detected stimulated photon echo

From Eq. (24) changing the integration variables with $t' = t - t_3$ and $t'' = t' + \tau - t_2$, the third contribution to the pump–probe absorption, S_{III}, is given by

$$\begin{aligned} S_{III}^{PL\text{-}PP}(\omega_1,\omega_2,\tau',\tau,\phi;\omega_{LO},\psi) = 2\,\mathrm{Re}\int_{-\infty}^{\infty} dt' \int_0^{\infty} dt_3 \int_{-\infty}^{t'+\tau} dt'' \int_0^{\infty} dt_1 \{ & [R_2(t_3,t'+\tau-t'',t_1)+R_3(t_3,t'+\tau-t'',t_1)] \\ & \times \chi(t_3-t_1)E_{LO}^{*}(t'+t_3)E_2(t')E_1(t'')E_1^{*}(t''+\tau'-t_1) \\ & \times \exp[i(\omega_{LO}-\omega_2)t'+i\psi+i(\omega_{LO}-\omega_{eg})t_3-i(\omega_1-\omega_{eg})t_1-i\phi]\}, \end{aligned} \tag{26}$$

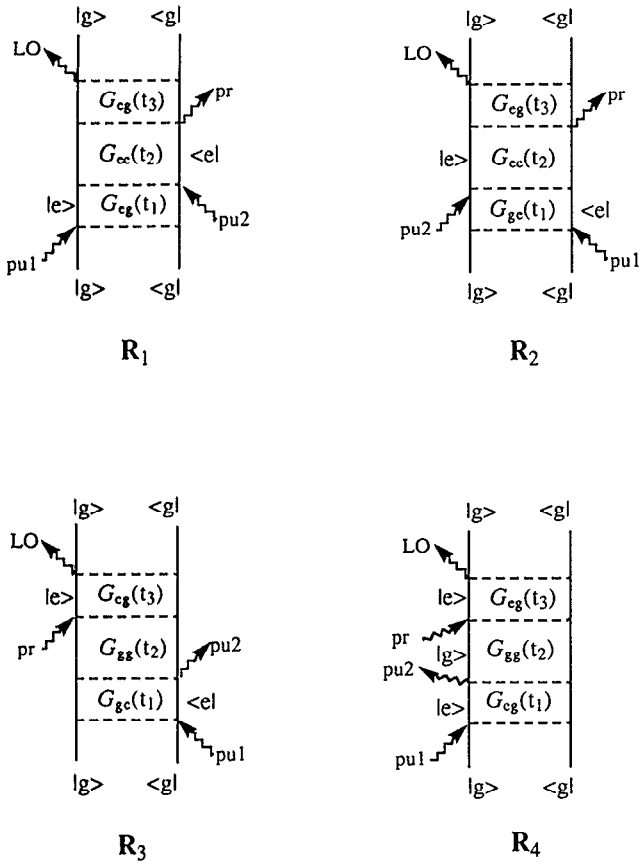

FIG. 3. Double-sided Feynman diagrams for phase-locked pump–probe absorption. The phenomenology of the diagrams was described in the caption of Fig. 2. Since it is assumed that the pulses are well separated, only the sequential interactions of the chromophore with three pulses (two pump and one probe pulses) are considered. pu1, pu2, pr, and LO denote the first pump, second pump, probe, and local oscillator pulses, respectively.

where the large inhomogeneous broadening limit, $\chi(t) \cong \delta(t)$, is assumed in Eq. (24). If we also invoke the impulsive limit for the two pump pulses, we obtain

$$S_{\mathrm{III}}^{\mathrm{PL\text{-}PP}}(\omega_1,\omega_2,\tau',\tau,\phi;\omega_{\mathrm{LO}},\psi) = \mathrm{Re}\{\exp[i(\omega_{\mathrm{LO}}-\omega_1)\tau' - i\phi + i\psi] \times \int_{-\infty}^{\infty} dt\,[R_2(\tau',t+\tau,\tau') + R_3(\tau',t+\tau,\tau')] \times E_{\mathrm{LO}}^{*}(t+\tau')E_2(t)\exp[i(\omega_{\mathrm{LO}}-\omega_2)t]\}. \quad (27)$$

Finally, when the probe pulse duration is short compared with the molecular nuclear dynamics, $E_2(t) \cong E_2\delta(t)$, and $\omega_1 = \omega_2 = \omega_{\mathrm{LO}}$, then

$$R_\alpha(\tau',t+\tau,\tau') \cong R_\alpha(\tau',\tau,\tau') \quad (\alpha = 2,3). \quad (28)$$

We thus obtain

$$S_{\mathrm{III}}^{\mathrm{PL\text{-}PP}}(\tau',\tau,\phi,\psi) \propto \mathrm{Re}\{\exp[i(\psi-\phi)][R_2(\tau',\tau,\tau') + R_3(\tau',\tau,\tau')]E_{\mathrm{LO}}^{*}(\tau')\}. \quad (29)$$

In comparison with Eq. (18), the three-pulse phase-locked pump–probe absorption contains an additional term, which is the envelope of the local oscillator field, $E_{\mathrm{LO}}^{*}(\tau')$. Thus, if the local oscillator pulse is of longer duration than the optical dephasing time, it is possible to study the optical dephasing process by measuring the third contribution (i.e., S_{III}) to the three-pulse pump–probe absorption. As shown in Eq. (29) the OHD phase-locked pump–probe absorption is an alternative approach for examining the fast optical dephasing process in condensed phases.

C. Comparison of PL-PP with conventional pump–probe and non-phase-locked approaches

The PL-PP method, through the separation of the two-pump interactions, makes possible the direct and linear measurement of optical dephasing. This is clearly in contrast with the conventional two-pulse pump–probe experiment. Since the two-pulse pump–probe absorption is given by the integration over the first (and third) time period, τ', which is the duration of the optical coherence state, it does not give any information on the optical dephasing process, unless the probe frequency spectrum is resolved.[15(c)]

The contributions I and II can be written as

$$S_{\mathrm{I}}(\tau+\tau') = \int_0^{\infty} dt S_{\mathrm{III}}^{\mathrm{PL\text{-}PP}}(t,\tau+\tau';\psi-\phi=0),$$

$$S_{\mathrm{II}}(\tau) = \int_0^{\infty} dt S_{\mathrm{III}}^{\mathrm{PL\text{-}PP}}(t,\tau;\psi-\phi=0), \quad (30)$$

when $E_2(t) = E_2\delta(t)$ and $\omega_1 = \omega_2 = \omega_{\mathrm{LO}}$.

Conventional two-pulse pump–probe measurement can show quantum beats that reflect a coherent superposition of vibrational states.[26(b)] In a recent three-pulse pump–probe experiment[29] using pulses with no optical phase control, it was demonstrated that the quantum beat signal can be manipulated by controlling the time interval τ_1. As τ_1 is varied, the vibrational beat signal can be periodically canceled or enhanced. When the optical phase is not controlled, the contribution S_{III} vanishes, and the signal is given by $S_{\mathrm{I}} + S_{\mathrm{II}}$. These measurements can be interpreted by noting that the quantum beat signal resulting from one pulse can be either in-phase or out-of-phase with those created by the other pulse. The manipulation of the beat signal in this case is purely *macroscopic* and does not represent *microscopic* control of the nuclear motions, as is obtained by controlling S_{III}, as discussed in this article. Any interference taking place between different Liouville space pathways occurs between different molecules and is therefore macroscopic; interference within a given pathway has to occur with the same molecule and is therefore microscopic. Phase-related optical pulse trains have also recently been applied to impulsive Raman experiments in solids where different phonon-modes of the material were selectively driven.[30,31]

VI. SPONTANEOUS LIGHT EMISSION USING PHASE-LOCKED PULSES

Spontaneous light emission (SLE) detection is usually viewed as a linear spectroscopic technique since the emitted light intensity is proportional to the incident light intensity. This view is formally correct. However, the theoretical description of SLE requires a quantum mechanical description of the emitted field. It can then be shown that the SLE signal is related also to the nonlinear polarization $P^{(3)}$. This fol-

lows from considering that the amplitude of the emitted light is to second order in the radiation matter interaction, first order with respect to the incident mode, and first order with respect to the emitted mode. The signal (amplitude squared) is thus fourth order, and its description in Liouville space will relate it to $P^{(3)}$.[26(a)]

The various contributions to the SLE can be separated into coherent (Raman) and sequential (fluorescence) contributions. There is a vast literature on the issue of separating Raman and fluorescence components in time domain and in frequency domain measurements.[32–40]

In this section we present the theoretical description of the spontaneous light emission induced by phase-locked pulse pairs studied by Scherer *et al.*[22] They used a phase-locked pulse pair to prepare the populations and vibrational coherences in either the ground or the excited states of the chromophore. The time-integrated total emission signal was recorded as a function of delay time between the two phase-locked pulses.

The pulse configuration of the phase-locked spontaneous light emission (PL-SLE) is shown in Fig. 1. The phase shift of the second optical pulse is maintained as ϕ with respect to the first pulse, and the two-pulse delay time is τ'. Here we formulate the spontaneous light emission signal created by a pair of phase-locked pulses. Since both the first and second fields contribute to the preparation of the optical coherences and population in either the ground or excited states, this signal that we are considering here is precisely identical to the signal measured by Scherer *et al.*[22] when it is time integrated. The incident field is treated classically and is given by

$$E(\mathbf{r},t) = E_1(t+\tau')\exp(i\mathbf{k}_1\mathbf{r} - i\omega_1 t) + E_2(t)\exp(i\mathbf{k}_1\mathbf{r} - i\omega_1 t - i\phi) + \text{c.c.} \quad (31)$$

Hereafter, the PL-SLE signal represents only the spontaneous light emission signal that results from one interaction from each field, E_1 and E_2.

Using the same nonlinear response functions defined in Eq. (5) and Eq. (74) of Ref. 26(a), the spontaneous emission signal can be written as

$$\begin{aligned} S^{\mathrm{PL}}_{\mathrm{SLE}}(\omega_1,\omega_2,\phi,\tau',t) = 2\,\mathrm{Re}\int_0^\infty dt_3\int_0^\infty dt_2\int_0^\infty dt_1 \{ & R_1(t_3,t_2,t_1)\chi(t_3+t_1)E_2^*(t-t_3-t_2)E_1(t+\tau'-t_3-t_2-t_1) \\ & \times\exp[i(\omega_2-\omega_{eg})t_3 + i(\omega_1-\omega_{eg})t_1 + i\phi] + R_2(t_3,t_2,t_1)\chi(t_3-t_1)E_2(t-t_3-t_2) \\ & \times E_1^*(t+\tau'-t_3-t_2-t_1)\exp[i(\omega_2-\omega_{eg})t_3 - i(\omega_1-\omega_{eg})t_1 - i\phi] + R_3(t_3,t_2,t_1)\chi(t_3-t_1) \\ & \times E_2(t-t_3)E_1^*(t+\tau'-t_3-t_2-t_1) \\ & \times\exp[i(\omega_2-\omega_{eg})t_3 - i(\omega_1-\omega_2)t_2 - i(\omega_1-\omega_{eg})t_1 - i\phi]\}. \end{aligned} \quad (32)$$

The phase-locked SLE signal observed experimentally[22] can be obtained by integrating the signal over t.

The first pulse creates an optical coherence. In the cases of the pathways 1 and 2, the second phase-locked pulse, whose phase factor is controlled, generates population in the excited state. Finally, the chromophore interacts twice with the outgoing fields which is the spontaneous fluorescence. On the other hand, the third pathway evolves via the population and vibrational coherence in the ground state since the second interaction is with the emitted (outgoing) field. The ground-state population is changed into an optical coherence state again by the interaction with the second incident pulse. Clearly this is related to the spontaneous Raman process.[26(a)] Double-sided diagrams representing the Liouville pathways, R_2 and R_3, are shown in Fig. 4.

Invoking the impulsive limit for the two pulses, Eq. (32) reduces to

$$\begin{aligned} S^{\mathrm{PL}}_{\mathrm{SLE}}(\omega_1,\omega_2,\phi,\tau',t) = {} & 2\,\mathrm{Re}\exp[i(\omega_1-\omega_{eg})\tau' + i\phi]\int_0^\infty d\tau R_1(t-\tau,\tau,\tau')\chi(t-\tau+\tau') \\ & \times\exp[i(\omega_2-\omega_{eg})(t-\tau)] + 2\,\mathrm{Re}\exp[i(\omega_{eg}-\omega_1)\tau' - i\phi] \\ & \times\int_0^\infty d\tau\{R_2(t-\tau,\tau,\tau')\chi(t-\tau-\tau')\exp[i(\omega_2-\omega_{eg})(t-\tau)] + R_3(t,\tau,\tau'-\tau)\chi(t-\tau'+\tau) \\ & \times\exp[i(\omega_2-\omega_{eg})(t+\tau)]\}. \end{aligned} \quad (33)$$

Assuming the large inhomogeneous broadening limit, $\chi(t)\cong\delta(t)$, we obtain a further simplified expression for the time-dependent phase-locked spontaneous light emission signal,

$$S^{\mathrm{PL}}_{\mathrm{SLE}}(\omega_1,\omega_2,\phi,\tau',t) = 2\,\mathrm{Re}\{\exp[i(\omega_2-\omega_1)\tau' - i\phi][R_2(\tau',t-\tau',\tau') + R_3(t,\tau'-t,t)]\}. \quad (34)$$

Here the first term associated with the first Liouville pathway R_1 in Eq. (33) does not contribute to the PL-SLE signal since $R_1(-\tau',t+\tau',\tau') = 0$ when $\tau' > 0$. Equation (34) can be understood as follows. If the detected emission frequency is identical to the incident field frequency, the phase shift, ϕ, determines whether the detected signal is produced by the real (i.e., $\phi = 0$; in phase) or imaginary (i.e., $\phi = \pi/2$; in quadrature) parts of the nonlinear response functions. Furthermore, time-gated detection of the spontaneous emission makes it possible to selectively measure each of the two contributions,

$R_2(\tau',t-\tau',\tau')$ and $R_3(t,\tau'-t,t)$. If $t \leqslant \tau'$, only $R_3(t,\tau'-t,t)$ contributes to the spontaneous emission since $R_2(\tau',t-\tau',\tau')$ vanishes by the causality condition. As mentioned before, the third pathway evolves via the population in the ground states. Therefore the short time ($t<\tau'$) emission is dominated by a spontaneous Raman process. However, the signal detected at $t>\tau'$ solely represents the fluorescence contribution from the second pathway, $R_2(\tau',t-\tau',\tau')$, since now $R_3(t,\tau'-t,t)$ vanishes through the causality condition.

The possible ways of detected signal can be summarized as

$$S_{\mathrm{SLE}}^{\mathrm{PL}}(\omega_1=\omega_2,\phi,\tau',t)=2\times\begin{pmatrix}\mathrm{Re}[R_3(t,\tau'-t,t)] & \text{for } \phi=0 & \\ & & \text{when } t\leqslant\tau' \\ \mathrm{Im}[R_3(t,\tau'-t,t)] & \text{for } \phi=\pi/2 & \\ \mathrm{Re}[R_2(\tau',t-\tau',\tau')] & \text{for } \phi=0 & \\ & & \text{when } t>\tau' \\ \mathrm{Im}[R_2(\tau',t-\tau',\tau')] & \text{for } \phi=\pi/2 & \end{pmatrix}. \tag{35}$$

As seen in Eq. (35), the phase factor in $S_{\mathrm{SLE}}^{\mathrm{PL}}(\omega_1=\omega_2,\phi,\tau',t)$ can be used to selectively measure the real and imaginary portions of each complex nonlinear response functions. To clarify the physical basis of Eq. (35), we present an illustration of the PL-SLE signal with respect to t in Fig. 5. The spontaneous Raman contribution is observed in the time range $0 \leqslant t < \tau'$, denoted as the Raman window in Fig. 5, whereas the fluorescence emission contributes to the PL-SLE signal at $t \geqslant \tau'$. The t dependence of R_3 is determined by the fast optical dephasing process, while that of R_2 is associated with the inverse lifetime of the excited electronic state. Furthermore, if $\tau' \to 0$ the R_3 (i.e., Raman) portion of the signal would occur during the duration of the second field. Since we do not include the vibrational coherences of the ground and excited states in the calculation, Fig. 5 does not show any oscillatory features. However, the magnitude of the total signal envelope including the vibrational coherence contributions would be represented by the signal shown in Fig. 5.

Since R_2 and R_3 represent the Liouville pathways associated with the excited and ground state dynamics during the time period t_2, vibrational coherences in the excited and ground electronic states can be created and appear as quantum beats in the PL-SLE signal. By measuring the R_2 and R_3 contributions to the PL-SLE signal as a function of the time t as seen in Fig. 5, we may extract the information on the vibrational dephasing process in the excited state from the R_2 contribution. If one measures the PL-SLE signal with respect to τ' for a constant t (with the restriction that $t<\tau'$), it is possible to study the vibrational dephasing process in the ground state, since the long-time portion of the signal, in this case, is associated only with the vibrational coherence of the ground state. This can be understood by carefully considering Eq. (35). The τ' dependence of R_3 is expected during the time period t_2, which is the duration of the population or vibrational coherence of the ground electronic state. On the other hand, the population or vibrational coherence of the excited state can be examined from the t-dependent measurement of the R_2 contribution to the PL-SLE signal.

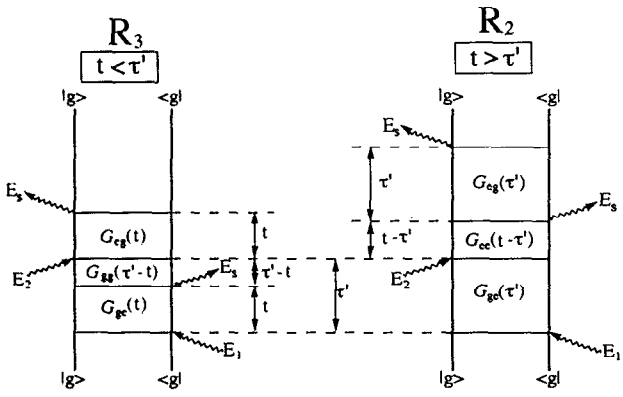

FIG. 4. Double-sided Feynman diagrams for PL-SLE. E_s is the scattered field mode. The last interaction, at time of detection (t), is with E_s. The signal requires two interactions with E_s, one with E_1 and one with E_2. R_2 represents a sequential fluorescence process (external fields first, scattered field later). R_3 represents a coherent Raman process with a mixed time ordering E_1, E_s, E_2, and finally E_s.

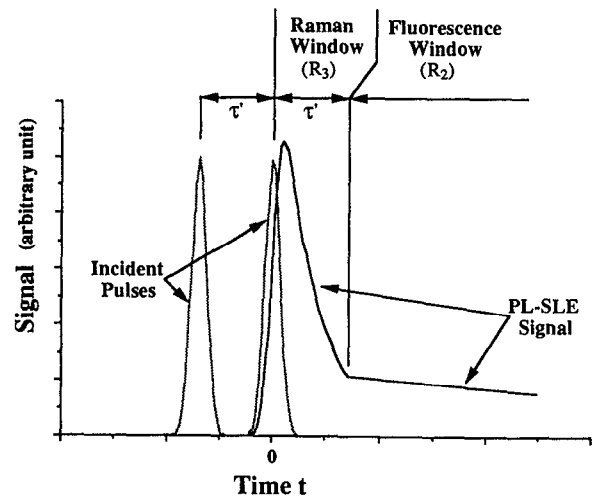

FIG. 5. PL-SLE signal, $S_{\mathrm{SLE}}^{PL}(\omega_1=\omega_2,\phi=0,\tau',t)$. τ' denotes the time delay between the two incident pulses. For simplicity, we use phenomenological dephasing constants to calculate the PL-SLE signal, the pulse shape is assumed a Gaussian, whose width is 1. The optical dephasing constant and the lifetime of the excited state are 4.7 and 35, respectively, compared with the pulse width.

In order to compare the phase-locked spontaneous light emission (PL-SLE) experiment with the photon echo and pump–probe experiments, we rewrite the heterodyne-detected stimulated photon echo (HSPE) signal as

$$S_{\mathrm{HSPE}}(t',t'',\psi) = [S^{\mathrm{PL}}_{\mathrm{SLE}}(\omega_1=\omega_2,\phi=\psi,\tau'=t',t=t'+t'') + S^{\mathrm{PL}}_{\mathrm{SLE}}(\omega_1=\omega_2,\phi=\psi,\tau'=t'+t'',t=t')]. \quad (36)$$

By using Eqs. (19), (21), and (29), the conventional photon echoes, two-pulse and phase-locked pump–probe absorption signals can be related to the phase-locked spontaneous light emission signal. This experimental technique can also be used to study optical dephasing processes and the dynamical processes of the condensed medium.

VII. SUMMARY

We have demonstrated how phase-locked optical pulses can be effectively used to investigate the optical dephasing processes in condensed media. We propose a new approach termed the heterodyne-detected stimulated photon echo spectroscopy that employs phase-locked pulses. The phase-locking approach in HSPE allows optical excitation (pump–probe) with a controllable relative optical phase between the pulses in a train, and detection with a phase-locked probe pair for linearized measurement of the third-order nonlinear response. The phase-sensitive detection is analogous to heterodyne detection in pump–probe absorption (or dichroism) measurements. The in-phase (in-quadrature) heterodyne-detected stimulated photon echo signal represents the real (imaginary) part of the corresponding nonlinear response functions [see Eq. (18)]. Measurement of the complete nonlinear response functions with the HSPE signal is sufficient to describe both two-pulse pump–probe absorption [Eq. (21)] and conventional photon echo signals [Eq. (19)].

By using a phase-locked pulse pair as a pump train, the three-pulse pump–probe absorption measurement would be useful in studies of the optical dephasing process in condensed media [see Eq. (29)]. The additional controllable time delay, τ', in the pump train and the precise phase relationship between the two pump pulses are the critical factors that enable study of the evolution of optical coherences. We have described the phase-locked excitation in combination with optical heterodyne detection.

Time-dependent detection of the spontaneous light emission signal using a phase-locked pulse pair enables detailed information on the individual nonlinear response functions [Eq. (35)] to be obtained. It is shown that the pure fluorescence and spontaneous Raman contributions to the SLE signal can be measured separately [Eq. (35)]. The relation of the PL-SLE approach to photon echoes and pump–probe absorption experiments is established in Eqs. (19), (21), and (36).

In the present paper the analogies between photon echoes, pump–probe, and spontaneous light emission measurements and their phase-locked variations, are presented in the impulsive and large inhomogeneous broadening limits. An important advantage of the present analysis, as compared to, e.g., calculations based on the solution of the Bloch equations, is that the conclusions and the relationships among the experimental techniques established here are very general since they are made without alluding to any specific model for the material system. The material response function can be modeled using a variety of methods including sums over states (for small size systems), stochastic models, dielectric response, Brownian oscillator models, semiclassical techniques, and molecular dynamic simulations.[26] An application of the present results using the multimode Brownian oscillator model for intramolecular and solvation modes will be made in the future.

ACKNOWLEDGMENTS

This work was supported by the National Science Foundation. M. C. thanks colleagues in Professor S. Mukamel's group for their hospitality during his stay at the University of Rochester.

[1] J. B. Birks, *Photophysics of Aromatic Molecule* (Wiley, New York, 1970).
[2] *Persistent Spectral Hole-Burning: Science and Applications*, edited by W. E. Moerner (Springer, Berlin, 1988).
[3] W. H. Hesselink and D. A. Wiersma, Phys. Rev. Lett. **43**, 1991 (1979); J. Chem. Phys. **73**, 648 (1980).
[4] (a) T. W. Mossberg, R. Kachru, A. M. Flusberg, and S. R. Hartmann, Phys. Rev. A **20**, 1976 (1979); (b) J. P. Gordon, C. H. Wang, C. K. N. Patel, R. E. Slusher, and W. J. Tomlinson, Phys. Rev. **179**, 294 (1969); (c) R. L. Shoemaker, Annu. Rev. Phys. Chem. **30**, 239 (1979).
[5] (a) T. Mossberg, A. Flusberg, R. Kachru, and S. R. Hartmann, Phys. Rev. Lett. **39**, 1523 (1977); (b) H. W. H. Lee, F. G. Patterson, R. W. Olson, D. A. Wiersma, and M. D. Fayer, Chem. Phys. Lett. **90**, 172 (1982).
[6] (a) J. B. W. Morsink, W. H. Hesselink, and D. A. Wiersma, Chem. Phys. **71**, 289 (1982); (b) S. Saikan, T. Nakabayashi, Y. Kanematsu, and A. Imaoka, J. Chem. Phys. **89**, 4609 (1988).
[7] (a) P. C. Becker, H. L. Fragnito, J. Y. Bigot, C. H. Brito-Cruz, R. L. Fork, and C. V. Shank, Phys. Rev. Lett. **63**, 505 (1989); (b) J. Y. Bigot, M. T. Portella, R. W. Schoenlein, C. J. Bardeen, A. Migus, and C. V. Shank, Phys. Rev. Lett. **66**, 1138 (1991).
[8] E. T. J. Nibbering, D. A Wiersma, and K. Duppen, Phys. Rev. Lett. **66**, 2464 (1991).
[9] R. F. Loring and S. Mukamel, Chem. Phys. Lett. **114**, 426 (1985); J. Chem. Phys. **83**, 2116 (1985).
[10] Y. J. Yan and S. Mukamel, J. Chem. Phys. **94**, 179 (1991).
[11] (a) B. M. Kharlamov, R. I. Personov, and L. A. Bykovskaya, Opt. Commun. **12**, 191 (1974); (b) Y. T. Mazurenko and V. S. Udaltsov, Opt. Spectrosc. **44**, 417 (1977); (c) M. J. Weber, J. Lumin. **36**, 179 (1987).
[12] (a) G. Shulte, W. Grond, D. Haarer, and R. J. Silbey, J. Chem. Phys. **88**, 679 (1988); (b) C. H. Brito-Cruz, R. L. Fork, W. H. Knox, and C. V. Shank, Chem. Phys. Lett. **132**, 341 (1986); (c) T. J. Kang, J. Yu, and M. Berg, J. Chem. Phys. **94**, 2413 (1991).
[13] K. A. Nelson and E. P. Ippen, Adv. Chem. Phys. **75**, 1 (1989).
[14] J. Chesnoy and A. Mokhtari, Phys. Rev. A **38**, 3566 (1988).
[15] (a) M. Mitsunaga and C. L. Tang, Phys. Rev. A **35**, 1720 (1987); (b) I. A. Walmsley, M. Mitsunaga, and C. L. Tang, *ibid.* A **38**, 4681 (1988); (c) I. A. Walmsley and C. L. Tang, J. Chem. Phys. **92**, 1568 (1990).
[16] (a) S. Saikan, Phys. Rev. A **38**, 4669 (1988); (b) T. Muramoto, S. Nakanishi, and T. Hashi, Opt. Commun. **36**, 409 (1981).
[17] W. S. Warren and A. H. Zewail, J. Chem. Phys. **78**, 2279 (1983).
[18] (a) N. F. Scherer, L. D. Ziegler, and G. R. Fleming, J. Chem. Phys. **96**, 5544 (1992); (b) C. Kalpouzos, D. McMorrow, W. T. Lotshaw, and G. A. Kenney-Wallace, Chem. Phys. Lett. **155**, 240 (1989); (c) D. McMorrow, W. T. Lotshaw, and G. A. Kenney-Wallace, IEEE J. Quantum Electron. QE-**24**, 443 (1988).
[19] H. L. Fragnito, J. Y. Bigot, P. C. Becker, and C. V. Shank, Chem. Phys. Lett. **160**, 101 (1989).

[20] R. F. Loring, Y. J. Yan, and S. Mukamel, J. Chem. Phys. **87**, 5840 (1987).
[21] N. F. Scherer, A. Ruggiero, M. Du, and G. R. Fleming, J. Chem. Phys. **93**, 856 (1990).
[22] (a) N. F. Scherer, R. J. Carlson, A. Matro, M. Du, A. J. Ruggiero, V. Romero-Rochin, J. A. Cina, G. R. Fleming, and S. A. Rice, J. Chem. Phys. **95**, 1487 (1991); (b) N. F. Scherer, A. Matro, L. D. Ziegler, M. Du, R. J. Carlson, J. A. Cina, and G. R. Fleming, J. Chem. Phys. **96**, 4180 (1992).
[23] R. Bavli, V. Engel, and H. Metiu, J. Chem. Phys. **96**, 2600 (1992).
[24] N. Bloembergen, *Nonlinear Optics* (Benjamin, New York, 1965).
[25] P. N. Butcher and D. Cotter, *The Elements of Nonlinear Optics* (Cambridge University, Cambridge, Mass., 1990).
[26] (a) S. Mukamel, Adv. Chem. Phys. **70**, 165 (1988); (b) S. Mukamel, Annu. Rev. Phys. Chem. **41**, 647 (1990).
[27] (a) S. Mukamel and R. F. Loring, J. Opt. Soc. Am. B **3**, 595 (1986); (b) Y. J. Yan and S. Mukamel, J. Chem. Phys. **89**, 5160 (1988).
[28] M. D. Levenson and S. S. Kano, *Introduction to Nonlinear Laser Spectroscopy* (Academic, New York, 1988).
[29] J. J. Gerdy, M. Dantus, R. M. Bowman, and A. H. Zewail, Chem. Phys. Lett. **171**, 1 (1990).
[30] A. M. Weiner, D. E. Leaird, G. P. Wiederrecht, and K. A. Nelson, Science **247**, 1317 (1990).
[31] Y. J. Yan and S. Mukamel, J. Chem. Phys. **94**, 997 (1991).
[32] B. R. Mollow, Phys. Rev. **188**, 1969 (1969); Phys. Rev. A **12**, 1919 (1975).
[33] D. L. Huber, Phys. Rev. **158**, 843 (1967).
[34] D. Lee and A. C. Albrecht, Adv. Infrared Raman Spectrosc. **12**, 179 (1985).
[35] A. B. Myers, R. A. Mathies, D. J. Tannor, and E. J. Heller, J. Chem. Phys. **77**, 3857 (1982).
[36] Y. R. Shen, Phys. Rev. B **9**, 622 (1974).
[37] T. Takagahara, E. Hanamura, and R. Kubo, J. Phys. Soc. Jpn. **43**, 802 (1977).
[38] (a) S. Mukamel, J. Chem. Phys. **82**, 5398 (1985); (b) J. Sue, Y. J. Yan, and S. Mukamel, J. Chem. Phys. **85**, 462 (1986).
[39] (a) F. A. Novak, J. M. Friedman, and R. M. Hochstrasser, in *Laser and Coherence Spectroscopy*, edited by J. I. Steinfeld (Plenum, New York, 1978), p. 451; (b) R. M. Hochstrasser and C. A. Nyi, J. Chem. Phys. **70**, 1112 (1979).
[40] Y. Fujimura and S. H. Lin, J. Chem. Phys. **74**, 3726 (1981).